# Electrical and thermal transport of composite fermions

V. C. Karavolas and G. P. Triberis
*Physics Department, Solid State Section, University of Athens, Panepistimiopolis, 15784 Zografos, Athens, Greece*

F. M. Peeters
*Department of Physics, University of Antwerp (UIA), B-2610 Antwerpen, Belgium*
(Received 14 July 1997)

The resistivity and the diffusion thermopower are calculated for a two-dimensional electron and hole gas at low temperatures in the fractional quantum Hall effect regime. The composite fermions picture enables us to use the integer quantum Hall effect and Shubnikov–de Haas conductivity models for a quantitative comparison with experiment. Satisfactory agreement with experiments on electron and hole gases is obtained. [S0163-1829(97)05647-6]

## I. INTRODUCTION

### A. Composite fermions

The quantum Hall effect, which occurs in two-dimensional electron and hole systems in strong magnetic fields, was first observed in 1980, opening a window to a remarkably interesting field of physics.[1] At very low temperatures and high magnetic fields an increasing number of Hall plateaus were observed corresponding to fractional filling factors with odd denominators. Laughlin[2] proposed a wave function that explained the behavior of the systems near filling factors with odd denominators.

A very promising approach to understand a system near even denominators is to attach to each particle an even number of ''flux quanta.'' In this way a quasiparticle named ''composite fermion'' (CF) was created. This is based on the idea of the transmutability of the statistics for particles in two-dimensional (2D) systems.[3] It is possible to introduce a Chern-Simons gauge field that interacts with the carriers resulting in a change of their statistics. The method is equivalent to the attachment of a ''magnetic-flux tube'' to each carrier. As a result, the quantum-mechanical properties of the quasiparticles are the same with those of the conventional particles.

Jain,[4,5] following this idea and attaching even numbers of flux quanta to each electron, successfully constructed the hierarchy of the fractional quantum Hall effect (FQHE) through the following equation:

$$\nu = \frac{\nu^*}{2m\nu^* \pm 1}, \tag{1}$$

where $\nu$ is the filling factor, $2m$ is the number of attached flux quanta, and $\nu^*$ a positive integer. The remarkable property of this idea is that instead of the FQHE for the actual carriers, at filling factor $\nu$, we study the integer quantum Hall effect (IQHE) for CF's, at filling factor $\nu^*$ As a result, the whole arsenal of ideas used to understand the IQHE are applicable to the FQHE.

Halperin, Lee, and Reed[6] showed that for an ideal sample with no impurity scattering precisely at $\nu = \frac{1}{2}$ and at various other filling factors with even denominators at $T=0$, a sharp Fermi surface exists similar to the one appearing at $B=0$. Kopietz and Castilla[7] showed that the quasiparticle picture for CF's, in the half-filled Landau level, remains valid even if the infrared fluctuations of the Chern-Simons gauge field are taken into account. These results improved the acceptance of the idea according to which we can understand the fermion (electron or hole) FQHE states as IQHE states at $\nu = 1/2m$ for CF's in an effective magnetic field $\Delta B$ given by

$$\Delta B = B - B_{1/2m} = \frac{2\pi\hbar c}{e}\frac{n_e}{\nu^*}, \tag{2}$$

where $n_e$ is the fermion concentration and $-e$ is the electron's charge.

### B. Transport coefficients

The thermoelectric properties of a two-dimensional electron gas (2DEG) have received a lot of attention in the last few years. A large number of experimental data for the thermopower are available for both zero and nonzero magnetic fields. However, the experimental situation is yet unclear. A large number of early data[8–13] show no indication of phonon drag, in agreement with the diffusion thermopower theories.[14–22] On the other hand, later studies, both experimental[23–26] and theoretical,[27–33] show a very large zero-field thermopower due to the domination of the phonon drag. Only recently, there is clear experimental evidence for the transition of the dominant mechanism from diffusion to phonon drag.[34]

However, the experimental data for the nondiagonal component of the thermopower $S_{xy}$ in the IQHE regime show a behavior similar to the diffusion thermopower, even for samples in which the diagonal part is clearly dominated by the phonon drag. The reason for this behavior is not well understood yet. A recent theory attributes this behavior to the acoustoelectric drag.[35] However, in the FQHE regime, it was found that the phonon-drag nondiagonal thermopower in the vicinity of the fractional states is proportional to $S_{xx}$ with a smaller component proportional to $dS_{xx}/dB$ superimposed on it.[36,37] Although the diffusion part of the thermopower is two orders of magnitude or more smaller than the phonon drag, at liquid-helium temperatures, recent calculations[38,39]

 

show that the diffusion part will again dominate the thermopower, at temperatures larger than 90 K. This is due to the fast decrease of the phonon mean free path caused by optical-phonon scattering.

On the other hand, in the last two years, experiments at very low temperatures (0.03–0.3 K) measured[40,41] the diffusion part of the thermopower and determined the temperature at which diffusion becomes dominant over the phonon drag.

These measurements have been performed in the FQHE regime, around filling factor, $\nu=\frac{1}{2}$ but the CF idea enables us to test the 2D models for diffusion thermopower with experiment, for the whole range of the effective fields.

In this work, we present calculations of the diffusion transport coefficients for a 2DEG and a two-dimensional hole gas, at low temperatures, near $\nu=\frac{1}{2}$. Different models for the conductivity will be used for the low and the high effective magnetic-field ranges.[42] For low fields, where the localization of the electrons does not play an important role, the model of Isihara and Smrčka,[43] as corrected by Coleridge *et al.*, will be used.[44]

For higher effective magnetic fields, a Gaussian density of states will be used, as proposed by Englert and co-workers.[45,46] Interesting results will be shown for the resistivity and the thermopower and we will discuss the interplay of the two models.

The present paper consists of the following: An introduction to the theory of the CF's (Sec. II A), a brief introduction to transport coefficients (Sec. II B), the models for the conductivity used in our calculations for small (Sec. II C), and large (Sec. II D) magnetic fields, are described in Sec. II. In Sec. III we present our results. In Secs. III A and III B we present our results for the resistivity and the thermopower, respectively, and we compare them with the experimental data.[47,48,40,49] Finally, in Sec. IV we present our conclusions.

## II. THEORY

### A. Composite fermions

The system under study consists of $N^-$ carriers (electrons or holes) moving on a plane $(x,y)$ in the presence of an external magnetic field $B=(0,0,B_z)$ perpendicular to the plane. We will consider only the case when the magnetic field is so high that all the carriers populate the lowest Landau level. Then we can ignore the spin contribution and write the Hamiltonian of the system as[3]

$$H=\sum_{j=1}^{N}\left[\frac{1}{2m^*}\left[\mathbf{p_j}+\frac{e}{c}\,\mathbf{A}(\mathbf{x_j})\right]^2+eA_0(\mathbf{x_j})\right]+\sum_{i>j}V(|\mathbf{x_i}-\mathbf{x_j}|), \tag{3}$$

where $\mathbf{A}$ is the electromagnetic vector potential, $m^*$ is the carriers effective mass, $\mathbf{p_j}$ is the momentum of each particle, $A_0$ is the scalar potential, and $V$ denotes the Coulomb potential generated by electron-electron interactions. An additional statistical vector potential $A_\mu$ $(\mu=0,1,2)$ can be introduced to change the statistics of the system. In this way the carriers are transformed to anyons. The action term of the statistical field is a Chern-Simons term,[3,50]

$$S_{\rm CS}=\int d^3x\,\frac{\theta}{4}\,\epsilon_{\mu\nu\lambda}A^\mu F^{\nu\lambda}, \tag{4}$$

where $\theta$ determines the statistics and $F^{\nu\lambda}$ is the field tensor for the statistical gauge field. In this way we obtain a Hamiltonian for the system which is identical to Eq. (3).[3,50,51] The Chern-Simons term results in a ''Gauss law'' for the particle density $j_0(x)$ and the statistical flux $B$,[3,51]

$$j_0(x)=\theta B(x). \tag{5}$$

For arbitrary values of $\theta$, Fradkin[51] showed that the system is a set of *anyons* with statistical angle

$$\delta=\frac{1}{2\theta}, \tag{6}$$

measured with respect to Fermi-Dirac statistics. Thus, for particular values of $\theta$, the system is again a set of fermions. These values are

$$\theta=\frac{1}{2\pi}\,\frac{1}{2n}, \tag{7}$$

and $n$ is an arbitrary integer. We can understand $\theta$ as the inverse of *the statistical flux per particle*. Thus, the above fermions are connected with $2\pi 2n$ which are understood as an even number of flux quanta attached to each particle.

Jain[4,5] proposed a wave function for the carriers of the form

$$\Psi(z_1,\ldots,z_{N^-})=\prod_{i,j}(z_i-z_j)^{m-1}\chi_1(z_1,\ldots z_{N^-}), \tag{8}$$

where $\chi_1$ is the wave function of a completely filled lowest Landau level, given by

$$\chi_1(z_1,\ldots,z_{N^-})=\prod_{i<j}(z_i-z_j)\exp\left[-\sum_{i=1}^{N^-}\frac{|z_i|^2}{4l^2}\right]. \tag{9}$$

The phases in the first factor in Eq. (8) can be understood as an even number $(m-1)$ of fluxes attached to each coordinate where a carrier is present. Lopez and Fradkin[3] showed that this approximation is the classical (mean-field) approximation of the above Chern-Simons description. They also showed that the above description leads to incompressible states.

A very important result from the theory is that the conductivities in the FQHE for the electrons and in the IQHE of the CF's are *added in parallel*.[3,6] This result is very crucial in our attempt for a quantitative comparison with experiment. Then the resistivity tensor can be written as

$$\rho=\begin{bmatrix}\rho_{xx} & -\rho_{xy}-\rho_{\rm CS}\\ \rho_{xy}+\rho_{\rm CS} & \rho_{xx}\end{bmatrix}, \tag{10}$$

where $\rho_{\rm CS}$ is the term in the nondiagonal resistivity, arising from the statistical potential,

$$\rho_{\rm CS}=\frac{2\pi\hbar s}{e^2}, \tag{11}$$

$\rho_{xy}$ is the CF's IQHE term, $\rho_{xx}$ is the diagonal resistivity of the CF's, and $s$ is the number of flux quanta attached to each

carrier. $\rho_{xx}$ and $\rho_{xy}$ are calculated using the same models as those we used to describe the carriers Shubnikov–de Haas (SdH) oscillations and the IQHE resistivity tensor, substituting only the carriers parameters with the CF ones and the actual magnetic field with the effective field given by Eq. (2).

### B. Transport theory

The basic equations that govern the response of a typical semiconductor to an external stimuli (for example an electric-field $\mathbf{E}$ or a temperature gradient $\nabla T$) are

$$\mathbf{J}=\sigma\mathbf{E_m}+L\nabla T, \tag{12a}$$

$$\mathbf{Q}=M\mathbf{E_m}+N_T\nabla T, \tag{12b}$$

where $\mathbf{E_m}$ is the electromotive force, $\mathbf{J}$ is the electric current density, $\mathbf{Q}$ is the thermal current density, $\sigma$ is the conductivity, and $L$, $M$, $N_T$ are the three rest transport coefficients.

For experimental convenience the above equations are transformed to

$$\mathbf{E_m}=\rho\mathbf{J}+S\nabla T, \tag{13a}$$

$$\mathbf{Q}=\pi\mathbf{J}-\kappa\nabla T, \tag{13b}$$

where $\rho$ is the resistivity, $S$ is the thermopower, $\pi$ is the Peltier coefficient, and $\kappa$ is the thermal conductivity. The relations between the resistivity $\rho$ and the thermopower $S$ with the original transport coefficients $\sigma$ and $L$ are

$$\rho=\sigma^{-1}, \tag{14a}$$

$$S=-\sigma^{-1}L. \tag{14b}$$

When a magnetic field is applied these coefficients become second rank tensors depending on the applied magnetic field. The following transport tensors have been derived from the Kubo formula by Smrčka and Středa[52] and they are given by

$$\sigma_{ij}=\int_{-\infty}^{\infty}\left(-\frac{\partial f(E)}{\partial E}\right)\sigma_{ij}(E)dE, \tag{15a}$$

$$L_{ij}=\frac{1}{eT}\int_{-\infty}^{\infty}\left(-\frac{\partial f(E)}{\partial E}\right)(E-E_F)\sigma_{ij}(E)dE, \tag{15b}$$

where $\sigma_{ij}(E)$ is the zero-temperature conductivity for $E=E_F$.

The thermopower tensor is given by[53]

$$S=-L\sigma^{-1}=-\rho L=\begin{pmatrix}-\rho_{xx}L_{xx}-\rho_{xy}L_{yx} & -\rho_{xy}L_{xx}+\rho_{xx}L_{yx}\\ \rho_{xy}L_{xx}-\rho_{xx}L_{yx} & -\rho_{xx}L_{xx}-\rho_{xy}L_{yx}\end{pmatrix}. \tag{16}$$

The temperature gradient $\nabla T$ initially causes a diffusion of the charge carriers that gives rise to a charge separation producing an electric field. This part of the thermopower is called the diffusion thermopower. On the other hand, the temperature gradient also produces a net flow of phonons parallel to $\nabla T$ and consequently a net phonon momentum. Part of this momentum is imparted to the electron system through electron-phonon scattering. Hence, an electric current is prompted to flow and an electric field builds up to oppose it.[27] This is responsible for the ''phonon drag'' part of the thermopower. Thus the thermopower is given by

$$S=S_d+S_g, \tag{17}$$

where $S_d$ is the diffusion part and $S_g$ is the phonon drag part.

### C. Small magnetic fields

In the low magnetic-field range the SdH oscillations of the resistivity $\rho_{xx}$, for a single subband, can be described by the model of Isihara and Smrčka,[43] which was corrected by Coleridge *et al.*[44] introducing different relaxation times. For the calculation of the conductivity a constant density of states (DOS) $g_0=m^*/\pi\hbar^2$ ($m^*$ is the effective mass) with a sinusoidal oscillating part superimposed has been used. The oscillating part of the DOS reflects the onset of the Landau levels and leads to the SdH oscillations of the magnetoconductivity. The conductivities $\sigma_{xx}$ and $\sigma_{xy}$ of a 2D system with a single occupied subband in a magnetic field $B$ are given by[44]

$$\sigma_{xx}=\frac{\sigma_0}{1+\omega_c^2\tau_s^2}\left(1+\frac{2\omega_c^2\tau_s^2}{1+\omega_c^2\tau_s^2}\frac{\Delta g}{g_0}\right), \tag{18a}$$

$$\sigma_{xy}=-\frac{\sigma_0\omega_c\tau_s}{1+\omega_c^2\tau_s^2}\left(1-\frac{1+3\omega_c^2\tau_s^2}{(1+\omega_c^2\tau_s^2)\omega_c^2\tau_s^2}\frac{\Delta g}{g_0}\right), \tag{18b}$$

where $\sigma_0$ is the zero-field conductivity, $\omega_c=eB/m^*$ is the cyclotron frequency, $\tau_s$ is the scattering time, and

$$\frac{\Delta g}{g_0}=2\sum_{r=1}^{\infty}e^{-\pi r/\omega_c\tau_q}\frac{rX}{\sinh(rX)}\cos\left(\frac{2\pi rE_F}{\hbar\omega_c}-\pi r\right) \tag{19}$$

is due to the oscillatory component of the DOS; $E_F=\pi\hbar^2n_e/m^*$ is the 2D Fermi energy, $\tau_q$ is the quantum lifetime, $X=2\pi^2kT/\hbar\omega_c$, and $k$ is the Boltzmann constant. This model is valid for low and intermediate fields such that $\omega_c\tau_q\leqslant 1$. Using the above expressions for $\omega_c$ and the definition of the mobility ($\mu=e\tau_s/m^*$) we can substitute in Eqs. (18a) and (18b) the term $\omega_c\tau_s$ with $\mu B$ while in Eq. (19) the term $\omega_c\tau_q$ can be expressed as $\mu_qB$. For larger magnetic fields the localization of the electrons away from the center of the Landau level starts to play an important role and the above model will no longer be applicable.

In Eqs. (18a) and (18b) both, the scattering time $\tau_s=m^*\sigma_0/e^2n_e$ and the quantum lifetime $\tau_q$ are present. In modulation-doped 2D systems they can differ by more than an order of magnitude.[54–57] The zero-field conductivity $\sigma_0=n_e\mu e$ is determined by the scattering time $\tau_s$, while the zero-field single-particle relaxation time or quantum lifetime $\tau_q$ is present in the oscillatory part of the DOS. The essential difference[44,55] between the two is that in the transport scattering rate, $1/\tau_s$, forward scattering is not counted and small-angle scattering receives a very small weight, as these scattering events have a small effect on the electron drift velocity. In the single-particle scattering rate $1/\tau_q$, however, every scattering event is equally important.

For $B=0$ the diffusion thermopower follows the equation

$$S_{xx}(B=0)=-\frac{\pi^2k^2T}{3e\sigma(E_F)}\left.\frac{d\sigma(E)}{dE}\right|_{E=\zeta}, \tag{20}$$

where $\zeta$ is the chemical potential measured relative to the bottom of the subband and $\sigma(E)$ is the conductivity for $E=\zeta$, written as

$$\sigma(E)=\frac{n_e(E)e^2\tau_s(E)}{m^*}. \tag{21}$$

Here, $n_e(E)=eEm^*/\pi\hbar^2$ is the particle density, when $E=\zeta$. A commonly used approximation in the literature[31,23,24,58] is to assume that

$$\tau_s(E)=\tau_0E^p, \tag{22}$$

where $p$ is a constant depending on the scattering mechanism. Then, the diffusion thermopower becomes

$$S_{xx}(B=0)=-\frac{\pi^2k^2T}{3E_Fe}(p+1). \tag{23}$$

Similarly, for the nondiagonal part at very low magnetic fields, we have[38]

$$S_{xy}=-p\frac{\pi^2k^2T}{3E_Fe}\frac{\omega_c\tau_s}{1+\omega_c^2\tau_s^2}. \tag{24}$$

For background impurity scattering, which is the dominant scattering mechanism for electrons at low temperatures, $p$ is of the order of unity.[58] Halperin, Lee, and Reed found that $p=0.5$ in the lowest Born approximation for the case of the static random magnetic field.[6] However, more recent calculations performed by Khveshchenko,[59] beyond the lowest Born approximation, gives $p=0.13$. From the peak in the $S_{xx}$ data at $B=B_{1/2}$ and using the above theoretically calculated value of $p=0.13$ we can obtain the value of the effective mass.

For higher magnetic fields, Fletcher, Coleridge, and Feng[34] found the oscillatory part of the diffusion thermopower to be given by

$$\Delta S_{xx}=\frac{2}{1+\mu^2B^2}\left(\frac{\pi k_B}{c}\right)\left(\frac{\partial(X/\sinh X)}{\partial X}\right)\times\exp\left(-\frac{\pi}{\omega_c\tau_q}\right)\sin\left(\frac{2\pi E_F}{\hbar\omega_c}-\pi\right). \tag{25}$$

For small fields, such that $\omega_c\tau_q<1$, we will use the Isihara-Smrčka model for the evaluation of the conductivities [Eq. (18)].

### D. Large magnetic fields

For sufficiently large magnetic fields applied to 2D systems, $\rho_{xx}$ becomes vanishingly small and $\rho_{xy}$ shows plateaus, in finite ranges of the magnetic field, when $E_F$ lies between two separated Landau levels. The quantized Hall resistance is attributed to immobile states which pin $E_F$ inside the gap between two Landau levels. In this way an integral number of levels can remain filled, in finite ranges of the magnetic field. These immobile states can be either localized states in the 2D layer or impurity states sufficiently close to the 2D layer. In both cases, the Hall current, carried by the mobile carriers, is equal to that carried by the total number of states in the filled Landau levels in the absence of these immobile states.[60] The conductivities of a 2D system are given by

$$\sigma_{xx}=\frac{e^2}{\pi^2\hbar}\sum_{N,s}\int dE\left(-\frac{\partial f(E)}{\partial E}\right)\times\left[\frac{\Gamma_N^{xx}}{\Gamma_{N,s}}\right]^2[\pi^2l^2\Gamma_{N,s}D_{N,s}(E)]^2, \tag{26a}$$

$$\sigma_{xy}=-\frac{e}{B}\sum_{N,s}\int dEf(E)D_{N,s}(E). \tag{26b}$$

Here, $f(E)$ is the Fermi-Dirac distribution function, $D_{N,s}(E)$ is the density of states for carriers in the Landau-level $N$ with spin $s$, $\Gamma_{N,s}$ is the Landau-level broadening, and $\Gamma_N^{xx}/\Gamma_{N,s}$ is a dimensionless factor that depends on the range of scatterers. The chemical potential $\zeta$ is determined through the condition of conservation of charge

$$n=\sum_{N,s}\int dEf(E)D_{N,s}(E). \tag{27}$$

The sum in the above equations runs over the single-particle states whose energies are given by

$$E_{N,s}=(n+\tfrac{1}{2})\hbar\omega_c. \tag{28}$$

The ratio $\Gamma_N^{xx}/\Gamma_{N,s}$ depends on the type of scattering. For short-range scattering[61]

$$\Gamma_N^{xx^2}=\Gamma_{N,s}^2(N+\tfrac{1}{2}). \tag{29}$$

Ando and Uemura[62] calculated the above ratio numerically for the case of a semielliptic DOS. They found that for long-range scattering the ratio $(\Gamma_N^{xx}/\Gamma_{N,s})^2$ is smaller than $(N+\frac{1}{2})$ and the difference from the short-range scattering result increases with the Landau level index $N$. In order to compare the high magnetic-field data with theory, a Gaussian form for the total DOS was used, namely,

$$D_{N,s}(E)=\frac{1}{2\pi l^2}\frac{1}{\sqrt{2\pi}\Gamma_{N,s}}e^{-(E-E_{N,s})^2/2\Gamma_{N,s}^2}, \tag{30}$$

where $l=\sqrt{\hbar/eB}$ is the magnetic length and $1/2\pi l^2$ is the available number of states in each Landau level. For short-range scattering, Ando, Fowler, and Stern[61] found

$$\Gamma_{N,s}^2=\frac{2}{\pi}e^2\frac{\hbar^2}{m^*2}\frac{B}{\mu_q}, \tag{31}$$

where $\mu_q=e\tau_q/m^*$ is the quantum mobility. In the center of the Landau levels the electron states are extended while those in the tail are localized and consequently do not contribute to the dispersive part of the conduction. In the phenomenological model of Englert,[45] the tails of the DOS are cut off at a characteristic energy in the $\sigma_{xy}$ calculation. This is achieved by using a Gaussian DOS of *extended states* with a width $\lambda_{N,s}<\Gamma_{N,s}$ of the form

$$D_{\lambda_{N,s}}(E)=\frac{1}{2\pi l^2}\frac{1}{\sqrt{2\pi}\lambda_{N,s}}e^{-(E-E_{N,s})^2/2\lambda_{N,s}^2}. \tag{32}$$

Substituting this in Eq. (26b), Eq. (26a) results in

$$\sigma_{xy}\frac{h}{e^2}=-\sqrt{2/\pi}\sum_{N,s}\int dE f(E)\,\frac{1}{\lambda_{N,s}}\,e^{-(E-E_{N,s})^2/2\lambda_{N,s}^2}, \tag{33}$$

and

$$\sigma_{xx}\frac{h}{e^2}=\tfrac{1}{4}\sum_{N,s}\Gamma_{N,xx}^2(N+\tfrac{1}{2})\int dE\left(\frac{\Gamma_{N,s}}{\lambda_{N,s}}\right)^2 \times\left(-\frac{\partial f(E)}{\partial E}\right)e^{-(E-E_{N,s})^2/\lambda_{N,s}^2}. \tag{34}$$

Here we introduced the factor $\Gamma_{N,xx}^2=(\Gamma_N^{xx}/\Gamma_{N,s})^2/(N+\frac{1}{2})$ which is equal to one in the case of short-range scattering. In the evaluation of the Fermi level the total DOS $D_{N,s}(E)$ is used. For $T=0$ K we have $-\partial f(E)/\partial E\sim\delta(E-E_F)$ and the integrals in Eqs. (33) and (34) can be evaluated analytically. Then $\sigma_{xx}$ consists of a series of Gaussian peaks with maxima at $E_F=E_N$. These peak values, $\sigma_{N,xx}$, can easily be obtained from Eq. (34) and they are given by

$$\sigma_{N,xx}=\frac{e^2}{h}\,\frac{1}{4}\,\frac{\Gamma_{N,s}^2}{\lambda_{N,s}^2}\,(N+\tfrac{1}{2})\Gamma_{N,xx}. \tag{35}$$

After a renormalization, necessary in order to have coincidence of our result with the one obtained using the semielliptic DOS, in the case of short-range scattering, the conductivity is given by

$$\sigma_{xx}\frac{h}{e^2}=\frac{1}{\pi}\sum_{N,s}\left(\frac{\Gamma_{N,s}}{\lambda_{N,s}}\right)^2(\Gamma_{N,xx})^2(N+\tfrac{1}{2})\int dE \times\left(-\frac{\partial f(E)}{\partial E}\right)e^{-(E_F-E_{N,s})^2/\lambda_{N,s}^2}. \tag{36}$$

The approximation of short-range scattering is clearly not satisfied in modulation-doped heterostructures. According to Ando, Fowler, and Stern,[61] it is obvious that, for long-range scattering, the peak transverse conductivity decreases rapidly with increasing scattering range. A number of theoretical investigations of the diffusion part of the thermopower have dealt with the disorder-free limit. With such an assumption the nondiagonal element of the thermopower $S_{xy}$ vanishes and the peaks of the diagonal element $S_{xx}$ appear at low temperatures. For $N>0$, $S_{xx}$ is given by[21]

$$S_{xx}=-\left(\frac{k}{e}\right)\frac{\ln 2}{N+\frac{1}{2}}. \tag{37}$$

It has been assumed that the broadening of the Landau level is $\Gamma_{N,s}>kT$. However, when the carriers are subjected to impurity scattering, $S_{xy}$ becomes finite and starts to oscillate passing through zero every time the Landau level is half filled. This results in a drop in the $S_{xx}$ maximum. However, these universal values of the diffusion thermopower $S_{xx}$ are an important indication which one of the diffusion or the phonon-drag term dominates the thermopower. For sets of data, for the half-filled Landau level, $S_{xx}$ has a value near that predicted from Eq. (37); the diffusion part is dominant. On the other hand, when the value of $S_{xx}$, for the half-filled Landau level, is orders of magnitude larger it means that the phonon-drag completely screens the diffusion term.

## III. RESULTS

### A. Resistivity: Theoretical results and comparison with experiment

In order to compare quantitatively our calculations with the experimental data we have to know the exact value of the CF effective mass for each sample. Halperin, Lee, and Reed[6] and d'Ambrumenil and Morf[63] calculated the effective mass and they found values around $m^*=0.3m_e$, where $m_e$ is the free-electron effective mass. They also found that this depends on the electron concentration. Halperin, Lee, and Reed also predicted that the CF effective mass is field dependent. Gee *et al.* also found that the effective mass depends on the angle and the confining potential in tilted fields.[64] Thus we have to use a different value for each sample according to the existing conditions. Measurements made by Leadley *et al.*[47] and Du *et al.*[48] showed the CF effective mass to be almost twice as large as theoretically expected. Du *et al.*[48] obtained the effective mass by extrapolation from their experimental data and they found that the CF effective mass diverges near $\nu=\frac{1}{2}$ in contrast with other measurements and recent theoretical calculations.[47,7]

In Fig. 1 we present the calculated resistivities in comparison with the experimental data of Leadley *et al.*[47] The mobility used in our calculations was obtained from the experimental $\rho_{xx}$ values at $\nu=\frac{1}{2}$. For CF's (at $B_{\rm eff}=0$, i.e., $B=B_{1/2}$)

$$\mu_{\rm CF}=(\rho_{xx}n_e e)^{-1}. \tag{38}$$

In our resistivity calculations we introduce $\mu_{\rm CF}$ to Eq. (18a). We have adopted the experimentally determined effective-mass equation[47]

$$m^*=m_0+\lambda_B\times B_{\rm eff}, \tag{39}$$

where $\lambda_B$ is a constant and $m_0$ is the effective mass at $B_{\rm eff}=0$. Leadley *et al.* gives for $m_0$ the value of $0.51m_e$. This value has been used in Fig. 1. The above zero effective-field value is about 8 times larger than the electron effective mass. This value is also about 60% higher than the theoretically calculated CF effective mass.[6,63] Leadley *et al.* found that $\lambda_B$ is 0.074. However, in order to reproduce correctly the slope of the $\rho_{xx}$, we have taken $\lambda_B$ to be 0.11.

It is obvious from Fig. 1 that the range of the validity of the Isihara-Smrčka model is limited in a small range around $B=B_{1/2}$. This model is incapable of explaining the $\rho_{xx}$ behavior at higher effective fields. On the other hand, the Englert model completely fails near $B=B_{1/2}$ but explains quite well the higher-field oscillations.

The same picture but over a much larger magnetic-field range is shown in Fig. 2 for the experimental results of Du *et al.*[48] In Fig. 2(a) we use the $m_0$ value reported by Du *et al.* for large effective fields ($m_0=0.9m_e$). In order to obtain the results presented in Fig. 2(b) we use the Abrumenil and Morf[64] equation for the $m_0$ at $\nu=\frac{1}{2}$, namely,

$$m_0=(0.36n_e^{1/2})m_e, \tag{40}$$

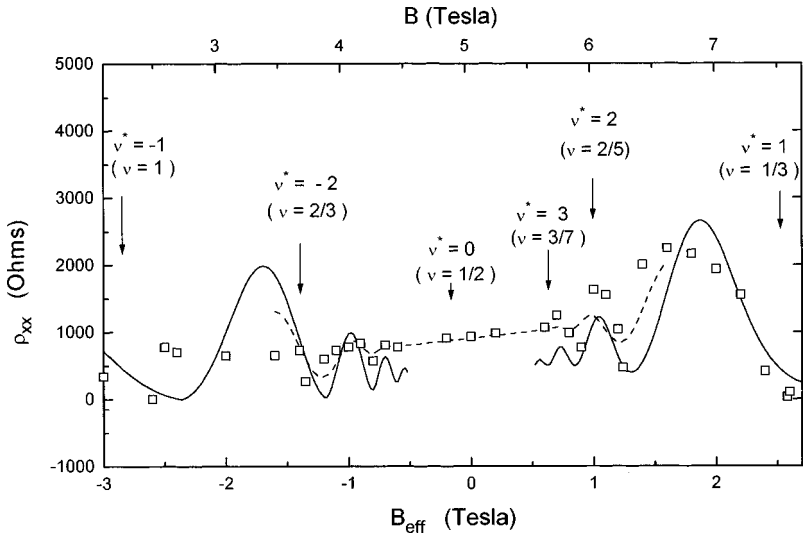


FIG. 1. Calculated $\rho_{xx}$ at 0.320 K compared with experimental data of Leadley *et al.* for different theoretical models. The squares represent the experimental data, the dashed line shows the theoretical calculations using the Isihara-Smrčka model, and the full line shows the theoretical calculations using the Englert model.

where, in this formula, $n_e$ is the composite particles concentration divided by $10^{15}$ m$^{-2}$. For larger effective fields Eq. (39) has been used for $\lambda_B=0.025$. This value is about 4 times smaller than the one used in Fig. 1. From Eq. (19) it is clear that the important factor in the oscillations is the quantum mobility. Thus, from these data we can deduce the quantum mobility value but not the effective mass. In Table I we see that $\mu_q$ is the same for Figs. 2(a) and 2(b) and this is the reason for the good agreement in both figures. The agreement between theory and experiment is better for the Abrumenil and Morf values of the effective mass and this is not surprising. A logarithmic correction due to the combined effect of the CF gauge interactions and the impurity scattering on the temperature dependence of the conductivity has been observed for which the analog for electrons at $B=0$ was negligible.[65,66] This has not been taken into account when Leadley *et al.* and Du *et al.* extrapolated their experimental data to obtain the effective-mass value. This observation explains the ''peculiar'' results of Du *et al.* for the effective mass.

The parameters used for the calculations are shown in Table I. Because of the fact that the scattering is long range the mobility is almost 6 times larger than the quantum mobility. This explains the value of $\Gamma^2_{N,xx}$ being 0.6. Ando, Fowler, and Stern found that this parameter is Landau-level dependent when the scattering is not of short range. In our attempt to limit the number of parameters used in our calculations we assumed that $\Gamma^2_{N,xx}$ has the same value at every Landau level. This is not artificial because the result of Ando, Fowler, and Stern shows that only the lowest Landau level for which the Englert model is not working well shows a constant $\Gamma^2_{N,xx}=1.0$ while the other Landau levels $\Gamma^2_{N,xx}$ values are between 0.5 and 0.8.

Again the Isihara-Smrčka model works quite well at low effective fields but shows some peculiar behavior ($\rho_{xx}<0$) at higher fields. The Englert model shows the opposite behavior. Thus one has to be quite careful which one of the models one uses, attempting to analyze experimental data or

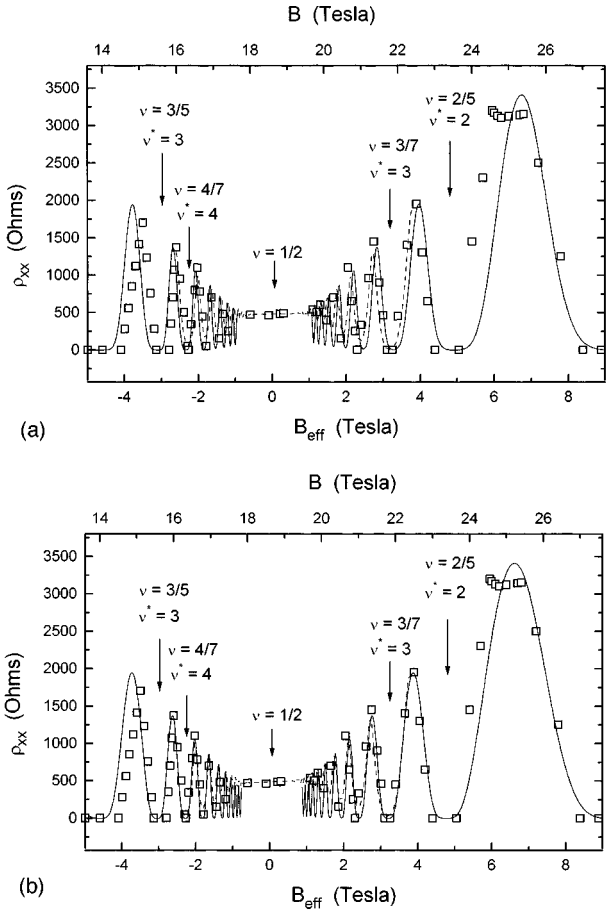


FIG. 2. Calculated $\rho_{xx}$ at 0.03 K compared with experimental data of Du *et al.* for different theoretical models. The squares represent the experimental data, the dashed line shows the theoretical calculations using the Isihara-Smrčka model, and the full line shows the theoretical calculations using the Englert model. In (a) we used the experimental value of the effective mass given by Du *et al.*, while in (b) we used the theoretical value of the effective mass given by Ambrumenil and Morf.

TABLE I. Parameters used for the calculation of the resistivities for the data of Leadley *et al.* (Figs. 1 and 4) and the data of Du *et al.* (Figs. 2 and 3).

| | Figs. 1, 4 | Fig. 2(a) | Figs. 2(b), 3 |
|---|---|---|---|
| | Fitting parameters | | |
| $\Gamma_{N,s}$ (meV) | $1.50\sqrt{B/\mu_q}$ | $1.0\sqrt{B/\mu_q}$ | $1.0\sqrt{B/\mu_q}$ |
| $\lambda_{N,s}$ (meV) | $0.25\sqrt{B/\mu_q}$ | $0.2\sqrt{B/\mu_q}$ | $0.25\sqrt{B/\mu_q}$ |
| $\Gamma_{N,xx}$ | 0.6 | 0.6 | 0.6 |
| | Physical parameters | | |
| $\mu$ ($m^2$/V s) | 12.1 | 5.74 | 5.7 |
| $\mu_q$ ($m^2$/V s) | 2.25 | 1.0 | 1.0 |
| $n_e$ ($\times 10^{15}$ $m^{-2}$) | 0.6 | 2.25 | 2.25 |

extract values of the effective mass. It is not allowed to use the Isihara-Smrčka model at high effective fields because its validity is rather limited.[44]

In Fig. 3 we present theoretical results of $\rho_{xy}+\rho_{cs}$ versus the magnetic field, using both models, for the same values of the parameter as those used to obtain Fig. 2. It is obvious that the Englert model reproduces quite well the plateaus in the nondiagonal resistivity while the Isihara-Smrčka model does not. The plateaus are at the correct positions and the $\rho_{xy}+\rho_{cs}$ has the expected values, frequently observed in experiments.[42]

In Fig. 4 the $E_F$ (thick full line) and the bottom energy of the first four CF Landau levels versus the effective magnetic field are plotted for the same values of the parameter values used in Fig. 1. The characteristic feature here is the effect on the Landau levels of the magnetic-field dependence of the effective mass. The Landau levels are no longer a straight line but are curved. The expected symmetry around $\nu=\frac{1}{2}$ has been destroyed by the large changes of the effective mass.

### B. Thermopower: Theoretical results and comparison with experiment

We have attempted to compare our theoretical calculations with two sets of experimental data of diagonal diffusion thermopower for holes.[49,40] Unfortunately, both sets lack measurements for the nondiagonal term of the thermopower to make our work more complete. In order to limit the number of parameters for the thermopower calculations we used a constant effective mass.

In Fig. 5 the diagonal component of the thermopower, $S_{xx}$, is shown for a system of holes near $\nu=\frac{1}{2}$, at $T=0.263$ K. We compare our theoretical results with the experimental data of Crump *et al.*[49] According to their experimental data the diffusion term of the thermopower dominates at $T=0.263$ K (or generally at $T<0.3$ K). The squares are the experimental data of Crump *et al.* and the crossed circles are the universal values of the $S_{xx}$ calculated from Eq. (37). The full line shows the theoretical results using the Englert model for large effective fields while the dashed line shows the theoretical results using the Isihara-Smrčka model. The latter fails completely to reproduce any of the oscillations observed in the $S_{xx}$ measurements. This is not surprising because of the effect of the first derivative of $X$ and the smearing effect of the $(1+\mu^2B^2)^{-1}$ in Eq. (25). However, the Isihara-Smrčka model shows a good agreement with the experimental data near the the peak at $B_{\rm eff}=0$. On the other hand, the high effective-field model reproduces quite well the oscillations when the CF Landau levels are half filled. This model fails completely near the peak at $\nu=\frac{1}{2}$. From Eq. (23), using for $p$ the value 0.13 calculated by Kveshchenko,[59] and using the experimental value of the peak $S_{xx}$, at $B_{\rm eff}=0$, we obtain $E_F$ and consequently for $n_e=0.9\times10^{15}$ $m^{-2}$ the value of the CF effective mass. This is found to be $1.45m_e$.

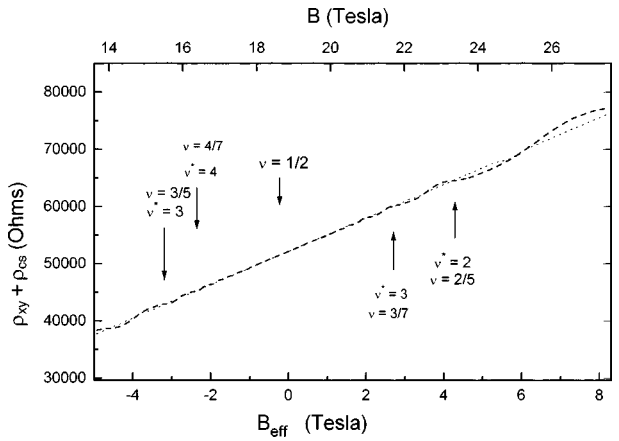


FIG. 3. Calculated $\rho_{xy}+\rho_{cs}$ at 0.03 K using the same values of the parameters as those used in Fig. 2(a). The dotted line shows the results for the Isihara-Smrčka model and the dashed line shows the results for the Englert model.

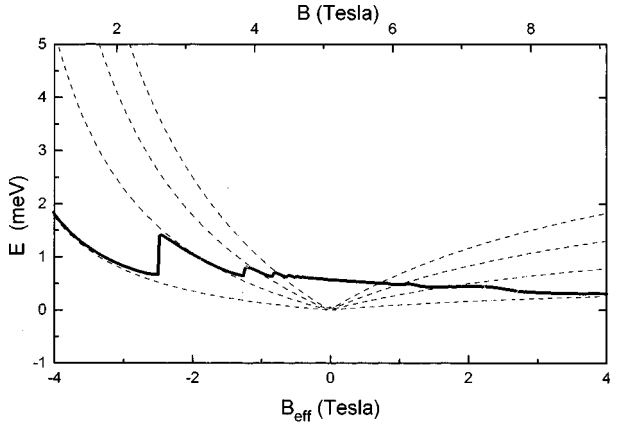


FIG. 4. The Fermi energy (full line) and the four lowest Landau levels of CFs at 0.320 K using the same values of the parameters as those used in Fig. 1.

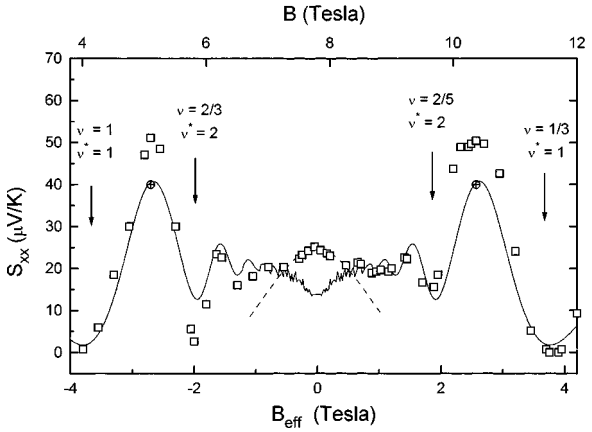


FIG. 5. Calculated $S_{xx}$ at 0.263 K compared with experimental data of Crump *et al.* for different theoretical models. The squares represent the experimental data, the dashed line shows the theoretical calculations using the Isihara-Smrčka model, the full line shows the theoretical calculations using the Englert model, and the crossed circles are the universal $S_{xx}$ values at half-filled Landau level.

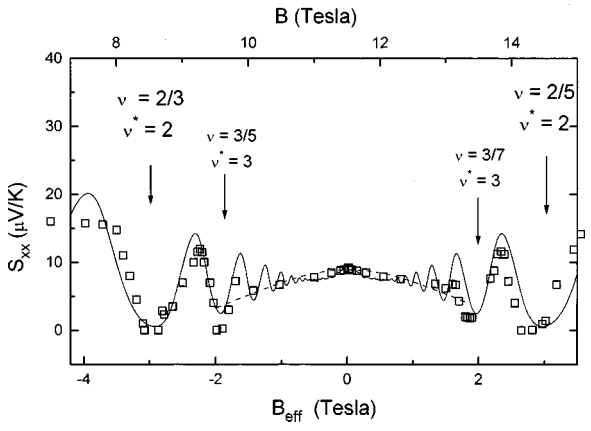


FIG. 6. Calculated $S_{xx}$ at 0.169 K compared with experimental data of Bayot *et al.* for different theoretical models. The squares represent the experimental data, the dashed line shows the theoretical calculations using the Isihara-Smrčka model, the full curve shows the theoretical calculations using the Englert model.

There is a problem with the height of the peaks, when a Landau level is half filled, but we believe that this has nothing to do with the diffusion term since this is also quite larger than the universal values of $S_{xx}$. The Englert model reproduces these universal values every time a CF level is half filled.

This problem does not appear in Fig. 6 where a similar plot as in Fig. 5 is shown, also for a hole system, at $T=0.169$ K. In Fig. 6 our theoretical results are presented and they are compared with the experimental data of Bayot *et al.*[40] They are found to be in very good agreement. Thus, it seems that the problem with the height of the peaks in Fig. 5 relies on the phonon-drag contribution which is significant at $T=0.263$ K but unimportant at lower temperatures such as $T=0.169$ K. Even at 0.3 K the diffusion thermopower dominates, in the case of hole carriers, in contrast with the electron systems, where the phonon drag starts to play the dominant role at lower temperatures than $T=0.169$ K. The Landau-level broadening we used for the extended states is magnetic-field dependent in contrast to the field-independent value given by Bayot *et al.* based on Zawadski and Lassnig.[17] They deduced a value around 0.13 meV while we obtain very good agreement with experiment using the value of $0.0027\times\sqrt{(B_{\rm eff}/\mu_q)}$ meV. The two values are equal at $B_{\rm eff}=3.0$ T. This means that our value is smaller than the one given by Bayot *et al.* for the whole range of the CF filling factors $\nu^*>2$. However, for the lower Landau levels measured, the two values are very near. The $\lambda_{N,s}$ values are almost identical in both figures. The values used for $\lambda_{N,s}$ show that the nature of scattering is of long range. The value of the effective mass, deduced from the experimental data of Bayot *et al.*, in the same way as before, is found to be equal to $1.2m_e$. Here we have to notice that the value of the effective-mass deduced from the data of Bayot *et al.* (for $n_e=1.35\times10^{15}$ m$^{-2}$) and our calculations, seems to be smaller than the value of the effective mass we calculated using the data of Crump *et al.* (for $n_e=0.9\times10^{15}$ m$^{-2}$). This is inconsistent with Eq. (40). We believe that this inconsistency is due to the fact that in Fig. 5 the contribution of the phonon drag to the thermopower, which is not dominant but significant, has not been taken into account and this leads to an artificial inconsistency as far as the values of the effective mass are concerned.

We also notice that using Eq. (25) we can deduce the value of the mobility, for each sample, from the slope of the $S_{xx}$ curve, at very low effective magnetic fields. These values are given in Table II.

TABLE II. Parameters used for the calculation of $S_{xx}$ for the data of Crump *et al.* (Fig. 5) and the data of Bayot *et al.* (Fig. 6).

| Index | Fig. 5 | Fig. 6 |
|---|---|---|
| | Fitting parameters | |
| $\Gamma_{N,s}$ (meV) | $0.019\sqrt{B/\mu_q}$ | $0.027\sqrt{B/\mu_q}$ |
| $\lambda_{N,s}$ (meV) | $0.002\sqrt{B/\mu_q}$ | $0.007\sqrt{B/\mu_q}$ |
| $p$ | 0.13 | 0.13 |
| | Physical parameters | |
| $\mu$ (m$^2$/V s) | 0.6 | 0.32 |
| $\mu_q$ (m$^2$/V s) | 0.22 | 0.12 |
| $n_e$ ($\times10^{15}$ m$^{-2}$) | 0.9 | 1.35 |

## IV. CONCLUSIONS

Our theoretical results show a very good quantitative agreement with the experimental data for the magnetoresistance (for electrons) and the diffusion thermopower (for holes) around filling factor $\nu=\frac{1}{2}$ and at temperatures lower than 0.3 K. For the interpretation of the experimental data we used two different models (Isihara-Smrčka and Englert) within the CF representation, and we investigated their range of validity.

The Isihara-Smrčka model reproduces quite well the transport coefficients behavior at the low effective-fields regime, where the Englert model fails. The latter model succeeds quite well at high effective magnetic fields, where the Isihara-Smrčka model fails, especially for the $S_{xx}$ and the $\rho_{xy}$.

We achieved a very good agreement of our theoretical results with the experimental data for the thermopower using a field-independent effective mass, which we were able to deduce from the zero effective magnetic-field value of $S_{xx}$. In contrast, for the diagonal resistivity, we had to use a field-dependent effective mass, in order to reproduce satisfactorily the slope of the curve. We were also able to deduce, from the slope of the $S_{xx}$ curve, at very low effective magnetic fields, the value of the mobility. There is still an open question as far as the phono-drag contribution is concerned and the behavior of other transport coefficients such as that of the thermal conductivity.

## ACKNOWLEDGMENTS

V.C.K. acknowledges the support of the Training Research and Mobility programme of the EC. F.M.P. was supported by the Flemish National Fund for Scientific Research.

[1] K. von Klitzing, G. Dorda, and M. Pepper, Phys. Rev. Lett. **45**, 494 (1980).
[2] J. R. B. Laughlin, Phys. Rev. Lett. **50**, 1395 (1983).
[3] A. Lopez and E. Fradkin, Phys. Rev. B **44**, 5246 (1991).
[4] J. K. Jain, Phys. Rev. Lett. **63**, 199 (1989).
[5] J. K. Jain, Phys. Rev. B **40**, 8079 (1989).
[6] B. I. Halperin, P. A. Lee, and N. Reed, Phys. Rev. B **47**, 7312 (1993).
[7] P. Kopietz and G. E. Castilla, Phys. Rev. Lett. **78**, 314 (1997).
[8] H. Obloh, K. von Klitzing, and K. Ploog, Surf. Sci. **142**, 236 (1984).
[9] H. Obloh, K. von Klitzing, K. Ploog, and G. Weinmann, Surf. Sci. **170**, 292 (1986).
[10] J. S. Davidson, E. D. Dahlberg, A. J. Valois, and G. Y. Robinson, Phys. Rev. B **33**, 2941 (1986).
[11] J. S. Davidson, E. D. Dahlberg, A. J. Valois, and G. Y. Robinson, Phys. Rev. B **33**, 8238 (1986).
[12] T. H. H. Vuong, R. J. Nicholas, M. A. Brummel, J. C. Portal, M. Razeghi, F. Alexandre, J. M. Masson, K. Y. Cheng, and A. Y. Cho, Surf. Sci. **170**, 298 (1986).
[13] T. H. H. Vuong, R. J. Nicholas, M. A. Brummel, J. C. Portal, F. Alexandre, J. M. Masson, and T. Kerr, Solid State Commun. **57**, 381 (1986).
[14] H. Oji, J. Phys. C **17**, 3059 (1984).
[15] H. Oji, Phys. Rev. B **29**, 3148 (1984).
[16] H. Oji and P. Streda, Phys. Rev. B **31**, 7291 (1985).
[17] W. Zawadski and R. Lassnig, Surf. Sci. **142**, 225 (1984).
[18] P. Streda, Phys. Status Solidi B **125**, 849 (1984).
[19] P. Streda and H. Oji, Phys. Lett. **102A**, 201 (1984).
[20] M. Johnson and S. M. Girvin, Phys. Rev. B **29**, 1939 (1984).
[21] S. M. Girvin and M. Johnson, J. Phys. C **15**, L1147 (1982).
[22] D. C. Cantrell, J. Phys. C **19**, L817 (1985).
[23] R. Fletcher, M. D'Iorio, W. T. Moore, and R. Stoner, J. Phys. C **21**, 2681 (1988).
[24] R. Fletcher, M. D'Iorio, A. S. Sachrajda, R. Stoner, C. T. Foxon, and J. J. Harris, Phys. Rev. B **37**, 3137 (1988).
[25] R. Fletcher, J. C. Maan, K. Ploog, and G. Weinmann, Phys. Rev. B **33**, 7122 (1986).
[26] C. Ruf, H. Obloh, B. Junge, E. Gmelin, K. Ploog, and G. Weinmann, Phys. Rev. B **37**, 6337 (1988).
[27] D. C. Cantrell and P. N. Butcher, J. Phys. C **19**, L429 (1986).
[28] D. C. Cantrell and P. N. Butcher, J. Phys. C **20**, 1985 (1987).
[29] D. C. Cantrell and P. N. Butcher, J. Phys. C **20**, 1993 (1987).
[30] S. S. Kubakaddi, P. N. Butcher, and B. G. Mulimani, Phys. Rev. B **40**, 1377 (1989).
[31] M. J. Smith and P. N. Butcher, J. Phys. Condens. Matter **1**, 1261 (1989).
[32] M. J. Smith and P. N. Butcher, J. Phys. Condens. Matter **1**, 4859 (1989).
[33] T. M. Fromhold, P. N. Butcher, G. Quin, B. G. Mulimani, J. P. Oxley, and B. L. Gallagher, Phys. Rev. B **48**, 5326 (1993).
[34] R. Fletcher, P. T. Coleridge, and Y. Feng, Phys. Rev. B **52**, 2823 (1995).
[35] V. I. Fal'ko, S. V. Meshkov, and S. V. Iordanskii, Phys. Rev. B **47**, 9910 (1993).
[36] U. Zeitler, R. Fletcher, J. C. Maan, C. T. Foxon, J. J. Harris, and P. Wyder, Surf. Sci. **305**, 91 (1994).
[37] U. Zeitler, J. C. Maan, P. Wyder, R. Fletcher, C. T. Foxon, and J. J. Harris, Phys. Rev. B **47**, 16 008 (1993).
[38] X. Zianni, P. N. Butcher, and M. J. Kearney, Phys. Rev. B **49**, 7520 (1994).
[39] R. Fletcher, J. J. Harris, C. T. Foxon, M. Tsaousidou, and P. N. Butcher, Phys. Rev. B **50**, 14 191 (1994).
[40] V. Bayot, E. Grivei, X. Ying, H. C. Manoharan, and M. Shaeygan, Phys. Rev. B **52**, R8621 (1995).
[41] B. Tieke *et al.*, Phys. Rev. Lett. **76**, 3630 (1996).
[42] M. van der Burgt, V. C. Karavolas, F. M. Peeters, J. Singleton, R. J. Nicholas, F. Herlach, J. J. Harris, M. Van Hove, and G. Borghs, Phys. Rev. B **52**, 12 218 (1995).
[43] A. Isihara and L. Smrčka, J. Phys. C **19**, 6777 (1986).
[44] P. T. Coleridge, R. Stoner, and R. Fletcher, Phys. Rev. B **39**, 1120 (1989).
[45] Th. Englert, in *Application of High Magnetic Fields in Semiconductor Physics II*, edited by G. Landwehr (Springer, Berlin, 1983), p. 165.
[46] Th. Englert, D. C. Tsui, A. C. Gossard, and Ch. Uihlein, Surf. Sci. **113**, 295 (1982).
[47] D. R. Leadley, R. J. Nicholas, C. T. Foxon, and J. J. Harris, Phys. Rev. Lett. **72**, 1906 (1994).
[48] R. R. Du, H. L. Stormer, D. C. Tsui, A. S. Yeh, L. N. Pfeiffer,

and K. W. West, Phys. Rev. Lett. **73**, 3274 (1994).
[49] P. A. Crump, B. Tieke, R. J. Barraclough, B. L. Gallagher, R. Fletcher, J. C. Maan, and M. Hennini, Surf. Sci. **361-362**, 50 (1996).
[50] F. Wilczek, *Fractional Statistics and Anyon Superconductivity* (World Scientific, Singapore, 1990).
[51] E. Fradkin, Phys. Rev. Lett. **63**, 322 (1989).
[52] L. Smrčka and P. Středa, J. Phys. C **10**, 2153 (1977).
[53] F. M. Peeters and P. Vassilopoulos, Phys. Rev. B **46**, 4667 (1992).
[54] M. A. Paalanen, D. C. Tsui, and J. C. M. Hwang, Phys. Rev. Lett. **51**, 2226 (1983); F. F. Fang, T. P. Smith III, and S. L. Wright, Surf. Sci. **196**, 310 (1988).
[55] J. P. Harrang, R. J. Higgins, R. K. Goodall, P. R. Jay, M. Laviron, and P. Delescluse, Phys. Rev. B **32**, 8126 (1985).
[56] U. Bockelmann, G. Abstreiter, G. Weimann, and W. Schlapp, Phys. Rev. B **41**, 7864 (1990).
[57] R. M. Kusters, F. A. Wittekamp, J. Singleton, J. A. A. J. Perenboom, G. A. C. Jones, D. A. Ritchie, J. E. F. Frost, and J.-P. André, Phys. Rev. B **46**, 10 207 (1992).
[58] V. C. Karavolas and P. N. Butcher, J. Phys. Condens. Matter **3**, 2597 (1991).
[59] D. V. Kveshchenko, Phys. Rev. B **54**, R14 317 (1996).
[60] S. M. Girvin, A. H. McDonald, and P. M. Platzman, Phys. Rev. B **33**, 2481 (1986).
[61] T. Ando, A. B. Fowler, and F. Stern, Rev. Mod. Phys. **54**, 437 (1982).
[62] T. Ando and Y. Uemura, J. Phys. Soc. Jpn. **36**, 959 (1974).
[63] N. d'Ambrumenil and R. Morf, Surf. Sci. **361-362,** 92 (1996).
[64] P. J. Gee, F. M. Peeters, S. Uji, H. Aoki, C. T. B. Foxon, and J. J. Harris, Phys. Rev. B **54**, R14 313 (1996).
[65] L. P. Rokhinson, B. Su, and V. I. Goldman, Phys. Rev. B **52**, 11 588 (1995).
[66] L. P. Rokhinson and V. I. Goldman, Phys. Rev. B **56**, R1672 (1997).